Biophysical Chemistry, 35 (1990) 271–285
Elsevier

BIOCHE 01430

Physicochemical characterization of substituted chromeno[4,3-*b*][1,5]benzodiazepine stereoisomers designed as cell membrane active antitumor agents

Walter Werner [a], Joachim Baumgart [a], Günter Burckhardt [a], Werner F. Fleck [a], Klaus Geller [a], Walter Gutsche [a], Helmut Hanschmann [a], Albrecht Messerschmidt [b,*], Wolfgang Römer [a], Dieter Tresselt [a] and Günter Löber [a]

[a] *Central Institute of Microbiology and Experimental Therapy and* [b] *Central Institute of Molecular Biology, Academy of Sciences of the German Democratic Republic, Jena, DDR-6900, G.D.R.*

Received 23 September 1989
Accepted 14 October 1989

Chromeno[4,3-*b*][1,5]benzodiazepine stereoisomer, substituted; NMR; CD; X-ray diffraction; Spectrophotometry; Fluorescence spectroscopy

As an alternative to naturally occurring pyrrolo[2,1-*c*][1,4]benzodiazepines (e.g., antramycin) which possess properties of DNA alkylation, we have designed several antileukemic chromeno[4,3-*b*][1,5]benzodiazepine derivatives with potential activity toward leukemia cell membranes and the cyclic nucleotide system. The *cis* and *trans* diastereoisomers were characterized by NMR. The absolute configurations of the enantiomers were established by X-ray diffraction and circular dichroism (CD) measurements. By means of absorption spectroscopy and determinations of fluorescence and fluorescence decay, it was found that the cancerostatically active compound (+)(6*aR*,13*aS*)-3,4-dimethoxy-10,11-dimethyl-6,6*a*,7,8,13,13*a*-hexahydrochromeno[4,3-*b*][1,5]benzodiazepine (ZIMET 54/79) and its biologically inactive (−) enantiomer (ZIMET 55/79) interact with liposomal membranes. At pH values of 6.0 and 7.3, the long-wave absorption bands of these agents showed weak bathochromic and hypochromic effects upon addition of neutral, and positively and negatively charged phosphatidylcholine and phosphatidylcholine/cholesterol liposomes. Such spectral changes are interpreted as resulting from the binding of both agents to phospholipid bilayers. Steady-state determinations using the membrane probe 1-anilino-8-naphthalenesulfonic acid (1,8-ANS) led to the observation of a small decrease in fluorescence intensity in the presence of either agent. Time-resolved measurements demonstrate that the mechanism of action of the agents occurs mainly through the partial displacement of probe molecules from regions of hydrophobic binding to areas of greater solvent accessibility. No significant differences in binding between the cancerostatically active and inactive enantiomers with liposomes (achiral systems) were detectable on the basis of spectrophotometric and fluorescence determinations. Cell membrane bound adenylate cyclase is stimulated by ZIMET 54/79, resulting in an increase of 103% in the level of cAMP in mouse L1210 leukemia cells. On examination of structure-activity relationships, it was found that the biological activity (leukemia L1210, P388, Lewis lung carcinoma, melanoma B16, increase in cAMP) is correlated with the particular configuration (6*aR*,13*aS*) and type of substituent at positions 3 and 4 of the benzo ring in the case of alkoxy groups and positions 10 and 11 for methyl groups. No activity was detected toward DNA/RNA using microbial test systems.

Correspondence address: W. Werner, Central Institute of Microbiology and Experimental Therapy, Academy of Sciences of the German Democratic Republic, Jena, DDR-6900, G.D.R.

* Present address: Max Planck Institute of Biochemistry, Structure Research, II, Am Klopferspitz, D-8033 Martinsried, F.R.G.

1. Introduction

Most antineoplastic agents attack DNA, RNA, proteins or their metabolites as alkylating compounds, antimetabolites or intercalators. An alter-

native approach to influencing the growth of malignant cells may be provided by agents that interact with cancer cell receptors, thereby modifying the activity of membrane-bound enzymes, such as adenylate cyclase. Cyclic nucleotides [1–4] appear to play an important role in the regulation of cell growth. Otten et al. [5,6] have shown via in vitro experiments that certain tumor cell lines, e.g., chicken fibroblasts infected with Rous sarcoma virus, can be retransformed and normalized morphologically by treatment with cyclic adenosine 3′,5′-phosphate (cAMP) or dibutyryl cAMP. Cell-density-dependent growth (contact inhibition of cells) appears to be restored and cultures grow as monolayers similarly to normal cells. The second messenger cAMP is capable of changing cell permeability, interacting with enzymes, transport proteins and histones, and influencing DNA metabolism. Growth inhibition could be brought about by increased cAMP levels in cells. Activation of adenylate cyclase or inhibition of the cAMP-specific phosphodiesterase are two possible routes by which the cAMP level in cells may be enhanced by chemical agents. Psychotropic drugs such as 1,4-benzodiazepines and phenothiazines [7] display manifold activities in the adenylate cyclase system, often reflected in the form of an increase in cAMP level.

In addition, psychotropic or central nervous system (CNS) active drugs with significant antitumor activities which do not involve cyclic nucleotides have been reported [8]. Pyrrolo-[2,1-*c*][1,4]benzodiazepines (e.g., antramycin) are well-known antibiotic metabolites isolated from *Streptomyces* strains which show clinical activity against gastrointestinal and breast tumors, lymphomas and sarcomas. They exert their antitumor effects through inhibiting DNA-directed RNA synthesis. Such inhibition results from covalent binding of the heterocyclic carbinolamine structure with the 2-amino group of guanine in DNA [9]. In contrast, our aim was to synthesize and characterize new 1,5-benzodiazepines that do not alkylate DNA or RNA, but do influence malignant cell growth by interacting with the receptor sites of tumor cell membranes or membrane constituents such as adenylate cyclase.

In order to characterize this new class of antineoplastic agents with low toxicity, we have evaluated the structure-activity relationships for stereoisomers of chromeno[4,3-*b*][1,5]benzodiazepines and essential substituents and determined their mechanism of action.

2. Materials and methods

2.1. Syntheses of chromeno[4,3-b][1,5]benzodiazepine derivatives

Werner et al. [10–14] synthesized several series of substituted chromeno[4,3-*b*][1,5]benzodiazepines (fig. 1 and tables 1–3). Condensation of substituted *o*-phenylenediamines with substituted 1,3-functionalized chroman-4-ones resulted in unsaturated heterocycles lacking biological activity in experimental tumor models. Finally, hydrogenation of one or two double bonds of the heterocycles yielded diastereoisomers and enantiomers of ring systems with two asymmetric carbon atoms. Some of the compounds exhibited antineoplastic properties. The separation of *cis* and *trans* configured diastereoisomers and the resolution of their optically active *cis* enantiomers have been carried out [10–14]. Tables 1 and 2 list the *cis* configured racemates and enantiomers while table 3 shows data on the related diastereomers with the *trans* configuration.

2.2. ^{1}H-NMR

^{1}H-NMR spectra were recorded at 100 MHz in C^2HCl_3 solution using a Tesla BS 497 spectrometer equipped with an FT adaptor.

2.3. X-ray diffraction

X-ray diffraction (Hilger & Watts four-circle automatic diffractometer) analysis was carried out with crystals of the (+)*cis* enantiomer ZIMET 54/79, using graphite-filtered MoKα radiation. (6*aR*,13*aS*)3,4-Dimethoxy-10,11-dimethyl-6,6*a*,7,8,13,13*a*-hexahydrochromeno[4,3-*b*][1,5]benzodiazepine hydrobromide methanolate: $C_{20}H_{24}N_2O_3 \cdot HBr \cdot CH_3OH$, colorless crystals, m.p. 199–201° C (corr.) (CH_3OH) [15].

2.4. Circular dichroism (CD)

CD spectra were recorded on a Cary 60 spectropolarimeter with a model 6001 CD attachment using 1 mm optical cells, and CH_3OH, C_2H_5OH or $CHCl_3$ as solvents [12].

2.5. Spectrophotometric and fluorescence measurements

2.5.1. Chemicals

Egg phosphatidylcholine (EPC) was prepared and purified according to a modification of the procedure of Singleton et al. [16]. Cholesterol (Chol), stearylamine (SA), dicetyl phosphate (DCP), 1-anilino-8-naphthalenesulfonic acid (1,8-ANS) and phosphate-buffered saline were obtained as commercial products of analytical grade.

2.5.2. Liposome preparation

Liposomes of the following compositions were used: EPC, EPC/Chol (molar ratio 1 : 1, neutral), EPC/Chol/DCP (molar ratio 7 : 5 : 2, negatively charged), EPC/Chol/SA (molar ratio 7 : 5 : 2, positively charged).

For vesicle preparation, pretreated lipid components were dispersed in phosphate-buffered saline (pH 7.2) and sonicated for 10 min (Branson Sonifier B-12, 75 J/s) under an inert gas and on ice. The stock solution contained 10^{-2} M lipid and was diluted before use. More detailed information is available in ref. 17.

2.5.3. Instrumentation

Spectrophotometric determinations were performed using a Specord UV/Vis spectrometer (VEB Carl Zeiss Jena, G.D.R.). Quantum-corrected fluorescence spectra were obtained by means of a Fica 55 type fluorometer. Time-resolved measurements were recorded by means of a nitrogen gas laser pulse fluorometer (LIF 200; Academy of Sciences of the G.D.R.) equipped with cut-off filters, a photodiode (rise time below 0.6 ns), and a BC1 280 boxcar averager for data acquisition. After correction [18], data were evaluated in terms of a double-exponential decay function using a least-squares reconvolution and fitting procedure (program ALAU [19]).

2.6. Cyclic nucleotide system

The effect of biologically active and inactive compounds on the cyclic nucleotide system was examined in vitro by employing a modification of the method of Thompson and Appleman [20] and in vivo by means of the competitive protein binding procedures of Gilman [21] and Thompson and Appleman [20] using $ABD2F_1$ hybrid mice bearing L1210 cells (cf. section 2.8). The agents were administered intraperitoneally.

2.7. Antimicrobial tests

The in vitro antimicrobial activity of *trans* (ZIMET 102/76, 32/86) and *cis* (ZIMET 54/79, 55/79, 15/87, 16/87) configured stereoisomers against a variety of different microorganisms was determined using a standardized agar plate diffusion assay seeded at 4×10^7 cells/ml per test plate (34 ml of nutrient agar). 0.1 ml suspensions of spores/cells were added to molten agar. Agar plates (15 cm in diameter) containing 12 wells (10 mm in diameter) were used to assess the antimicrobial activity of each compound. Standards of *cis* and *trans* diastereoisomers were prepared as stock solutions in dimethyl sulfoxide (DMSO) at a concentration of 5 mg/ml. 50-μl samples of the compounds at different concentrations were placed in the wells and after diffusion at room temperature for 1 h, all test plates were incubated for 16 h at 37 °C. As special test models the prophage induction and BIP [22] tests were used.

2.8. Tumor and animal models

2.8.1. Mice

DBA/2 Jena and C57BL/6 Jena inbreds, (AB/Jena × DBA/2 Jena) F_1-hybrids ($ABD2F_1$) and (C57BL/6 Jena × DBA/2 Jena) F_1-hybrids ($B6D2F_1$) of either sex from this institute's animal breeding unit (SPF) were used at 6–8 weeks of age (17–21 g body weight). The housing conditions have been described previously [23–25].

2.8.2. Tumors and experiments

The tumor lines, cryoconserved in liquid nitrogen, were grown in animals of the syngeneic in-

bred strain for one passage and then used for experiments on hybrids. Tumor lines (abbreviation) and mouse strains for experiments were: leukemia L1210 (L1210), $B6D2F_1$, $ABD2F_1$; leukemia P388 (P388), $B6D2F_1$, $ABD2F_1$; melanoma B16 (B16), $B6D2F_1$; Lewis lung carcinoma (LLC), $B6D2F_1$; lymphoma (ABDt2), $ABD2F_1$.

Details of the transplantation techniques employed have appeared elsewhere [23,26].

Tumor inoculation was performed on day 0. Treatment was initiated on day 1. The end point of experiments was generally day 30 except in LLC where experiments were finished on day 23. The effects were expressed as increased life span (ILS) in survival experiments (L1210, P388, B16) or tumor weight inhibition (TWI) with LLC. In vitro activity was determined by the method of Jungstand [27] which depends on the inhibition of proliferation of an L1210 cell culture line.

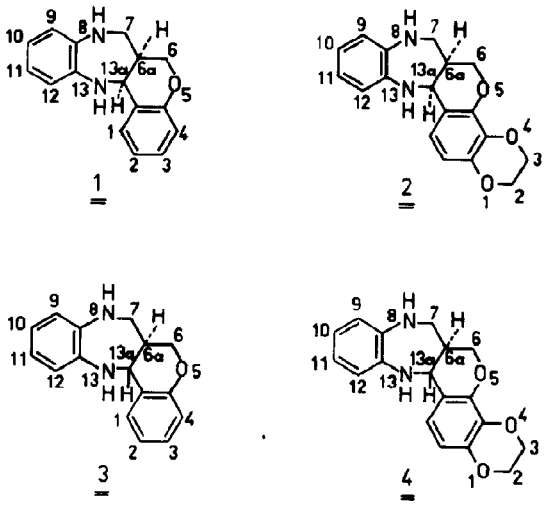

Fig. 1. Formulae of the basic structures of the diastereomers (6*aR*,13*aS*)-6,6*a*,7,8,13,13*a*-hexahydrochromeno[4,3-*b*]-[1,5]benzodiazepine (**1**, *cis*-HHCB); (6*aR*,13*aS*)-2,3,6,6*a*,7,8,13,13*a*-octahydro[1′,4′]dioxino[2′,3′:7,8]chromeno-[4,3-*b*][1,5]benzodiazepine (**2** *cis*-OHDCB); (6*aR*,13*aR*)-6,6*a*,7,8,13,13*a*-hexahydrochromeno[4,3-*b*][1,5]benzodiazepine (**3**, *trans*-HHCB);(6*aR*,13*aR*)-2,3,6,6*a*,7,8,13,13*a*-octahydro-[1′,4′]dioxino[2′,3′:7,8]chromeno[4,3-*b*][1,5]benzodiazepine (**4**, *trans*-OHDCB).

3. Results

3.1. Evaluation of the cis and trans diastereomeric configurations

The *cis* and *trans* configurations of the compounds shown in fig. 1 and tables 1–3 can be discriminated by ^{1}H-NMR spectra [10]. The vicinal coupling constants between 6*a*-H and 13*a*-H establish the relative configuration. In the case of compounds with *cis* configuration (tables 1 and 2), estimation of $J_{6a\text{-H},13a\text{-H}}$ is simple. A doublet signal within the range 4.50–4.80 ppm with a splitting of 3.5 Hz results from the 13*a* proton. This splitting remains invariant after hydrogen-deuterium exchange (NH coupling does not participate) and therefore directly represents the vicinal coupling $J_{6a\text{-H},13a\text{-H}} = 3.5$ Hz. For compounds with the *trans* configuration (table 3), however, the corresponding signal is masked by other absorption bands. Therefore, we determined $J_{6a\text{-H},13a\text{-H}}$ as follows. To a C^2HCl_3 solution of the compound under investigation, a few drops of trichloroacetyl isocyanate were added. Both NH groups of the molecule consequently reacted with the reagent and yielded the corresponding ureas. During the process of forming the derivatives, no change in the linking of the heterocyclic rings is possible. However, the 13*a*-H signal shifts downfield and appears within the range 5.40–5.80 ppm, where no other signals are present. This signal displays a doublet structure with a splitting of 11.5 Hz ($J_{13a\text{-H},6a\text{-H}} = 11.5$ Hz). The unambiguous assignment of the coupling constants $J_{6a\text{-H},13a\text{-H}} =$ 3.5 and 11.5 Hz to the *cis* and *trans* configuration, respectively, resulted from studies of Dreiding's models. For the *trans* configuration (and for all possible conformations) the only dihedral angles possible lie between 150 and 180°.

On the other hand, for the *cis* configuration (and likewise for all possible conformations) dihedral angles spanning the range 0–60° were found. Because the Karplus relation required coupling constants of 8–12 Hz for dihedral angles greater than 150°, the value $J_{13a\text{-H},6a\text{-H}} = 3.5$ Hz is impossible for the *trans* configuration. However, the above-mentioned assignment (*cis* configura-

Table 1

ZIMET compounds derived from *cis*-HHCB (fig. 1, **1**) substituents attached to image **1**, reflected image *ent-1* or racemic images *rac-1*; relative and absolute configurations, antitumor activity in vitro (yes, significant inhibition of cell growth (≥ 60% after 24 h incubation of test samples)) and in vivo (cf. table 8; n.t., not tested)

ZIMET no.	Substituents	Images	Configurations		Antitumor activity		
			Relative	Absolute	In vitro	Inactive	In vivo
					L1210	Active	Inactive
31/76	3,4-dimethoxy	**rac-1**	(±)*cis*		no		L1210
89/79	3,4-dimethoxy	**1**	(+)*cis*	(6*aR*,13*aS*)	no		n.t.
88/79	3,4-dimethoxy	**ent-1**	(−)*cis*	(6*aS*,13*aR*)	no		L1210, P388
52/80	10,11-dimethyl	**1**	(+)*cis*	(6*aR*,13*aS*)	no		n.t.
14/89	10,11-dimethyl	**ent-1**	(−)*cis*	(6*aS*,13*aR*)	no		n.t.
71/78	3-methoxy-10,11-dimethyl	**rac-1**	(±)*cis*		no		L1210, P388
20/78	3,4,10,11-tetra methoxy	**rac-1**	(±)*cis*		yes		L1210, P388
101/76	3,4-dimethoxy-10,11-dimethyl	**rac-1**	(±)*cis*		yes	L1210, P388, LLC	
54/79	3,4-dimethoxy-10,11-dimethyl	**1**	(+)*cis*	(6*aR*,13*aS*)	yes	L1210, P388, B16, LLC, $ABDt_2$	
55/79	3,4-dimethoxy-10,11-dimethyl	**ent-1**	(−)*cis*	(6*aS*,13*aR*)	no		L1210, P388

tion, $J = 3.5$ Hz; *trans* configuration, $J = 11.5$ Hz) is in good agreement with Dreiding's model and the Karplus relation.

3.2. Absolute configuration of (6aR,13aS)3,4-dimethoxy-10,11-dimethyl-6,6a,7,8,13,13a-hexahydrochromeno[4,3-b][1,5]benzodiazepine (ZIMET 54/79) as determined by X-ray diffraction

The crystal and molecular structure of the hydrobromide methanolate of the antileukemic ZIMET 54/79 (**1**; fig. 1 and table 1) was elucidated by performing single-crystal structure analysis. Detailed results have been reported by Messerschmidt and Werner [15]. The absolute configuration was determined unambiguously by the application of anomalous dispersion effects. It was found that ZIMET 54/79 possesses the (6*aR*, 13*aS*) configuration as shown in fig. 2. The intramolecular dimensions (fig. 3) are within the expected ranges. The two benzo rings are flat, as indicated by the torsion angles ($\leq 3.1°$). The pyrano and diazepine rings are *cis*-fused. The diazepine ring shows a C-13*a*/α-C-7/β-twist-boat conformation as indicated by the ΔC_2(C-6*a*) asymmetry parameter (figs. 3 and 4) [28]. The pyrano ring has a C-6*a*/α-C-6/β-half-chair conformation. Fig. 7 provides a view of the α-side of the molecule. The 3-methoxy substituent is synperiplanar to C-2 forming a torsion angle, C-2-C-3-O-3-C-31, of 2.1°. The 4-methoxy group is nearly synclinal to C-4*a* with a corresponding torsion angle, C-4*a*-C-4-O-4-C-41, of −71.8°.

3.3. Determination of the absolute configuration of cis-HHCB and cis-OHDCB derivatives by CD

The X-ray structure of ZIMET 54/79 (hydrobromide methanolate) was used to determine the absolute configuration of related enantiomeric partially hydrogenated chromeno[4,3-*b*][1,5]benzodiazepines and [1′,4′]dioxino[2′,3′ : 7,8]chromeno-[4,3-*b*][1,5]benzodiazepine derivatives (tables 1 and 2). By means of CD measurements of the enantiomeric pairs and comparison with the Cotton effects (table 4) of ZIMET 54/79 ((6*aR*,13*aS*) configuration) (fig. 4), the absolute configuration of ZIMET 52/80, 89/79 and 15/87 was determined to be (6*aR*,13*aS*) while that of ZIMET

Table 2

ZIMET substances derived from *cis*-OHDCB (fig. 1, **2**), substituents attached to image **2**, reflected image **ent-2** or racemic images **rac-2**; relative and absolute configurations antitumor activity in vitro (yes, significant inhibition (table 1)) and in vivo (cf. table 8)

ZIMET no.	Substituents	Images	Configurations		Antitumor activity		
			Relative	Absolute	In vitro	In vivo	In vivo inactive
					L1210	Active	Inactive
31/86	10,11-dimethyl	**rac-2**	(±)*cis*		yes	P388	
15/87	10,11-dimethyl	**2**	(+)*cis*	(6*aR*,13*aS*)	yes	P388, LLC	
16/87	10,11-dimethyl	**ent-2**	(−)*cis*	(6*aS*,13*aR*)	no		P388

55/79, 88/79, 14/89 and 16/87 (fig. 5) was found to be (6*aS*,13*aR*). The Cotton effects of other related compounds have been described by Werner and Burckhardt [12].

3.4. Absorption and fluorescence spectroscopy of the interaction of ZIMET 54/79 and 55/79 with liposomal membranes

The series of experiments described below represents our efforts to obtain evidence in support of the potential binding affinity of this class of compounds to the lipid-bilayer matrix of biomembranes. Using liposomal membranes as models of biomembranes and 1,8-ANS as a fluorescent membrane probe, we attempted to demonstrate interactions of ZIMET 54/79 and its antineoplastically inactive enantiomer 55/79 with different types of liposomes by means of absorption and fluorescence spectroscopy including fluorescence decay measurements.

Since monomer binding of substances to mac-

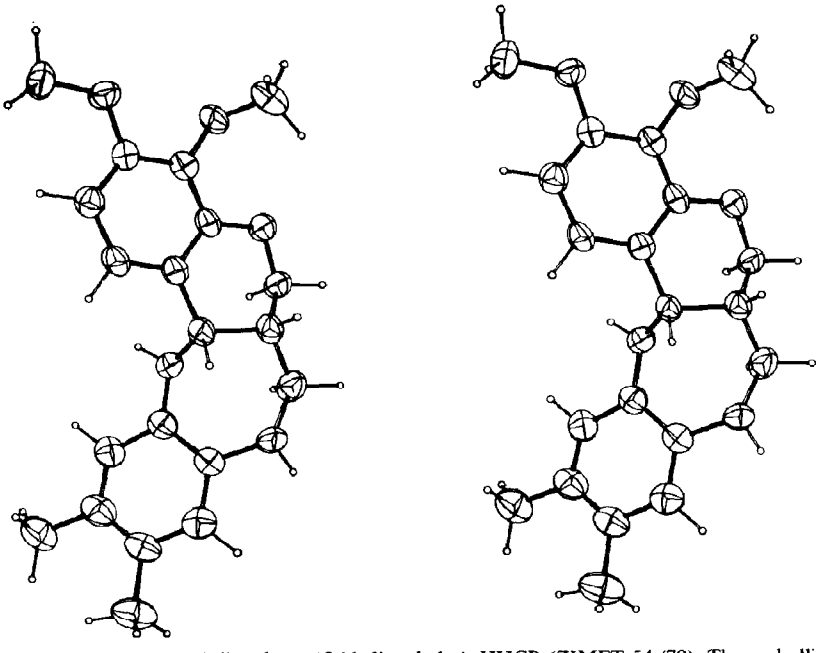

Fig. 2. ORTEP plot [39] of (6*aR*,13*aS*)3,4-dimethoxy-10,11-dimethyl-*cis*-HHCB (ZIMET 54/79). Thermal ellipsoids are scaled to 50% probability level.

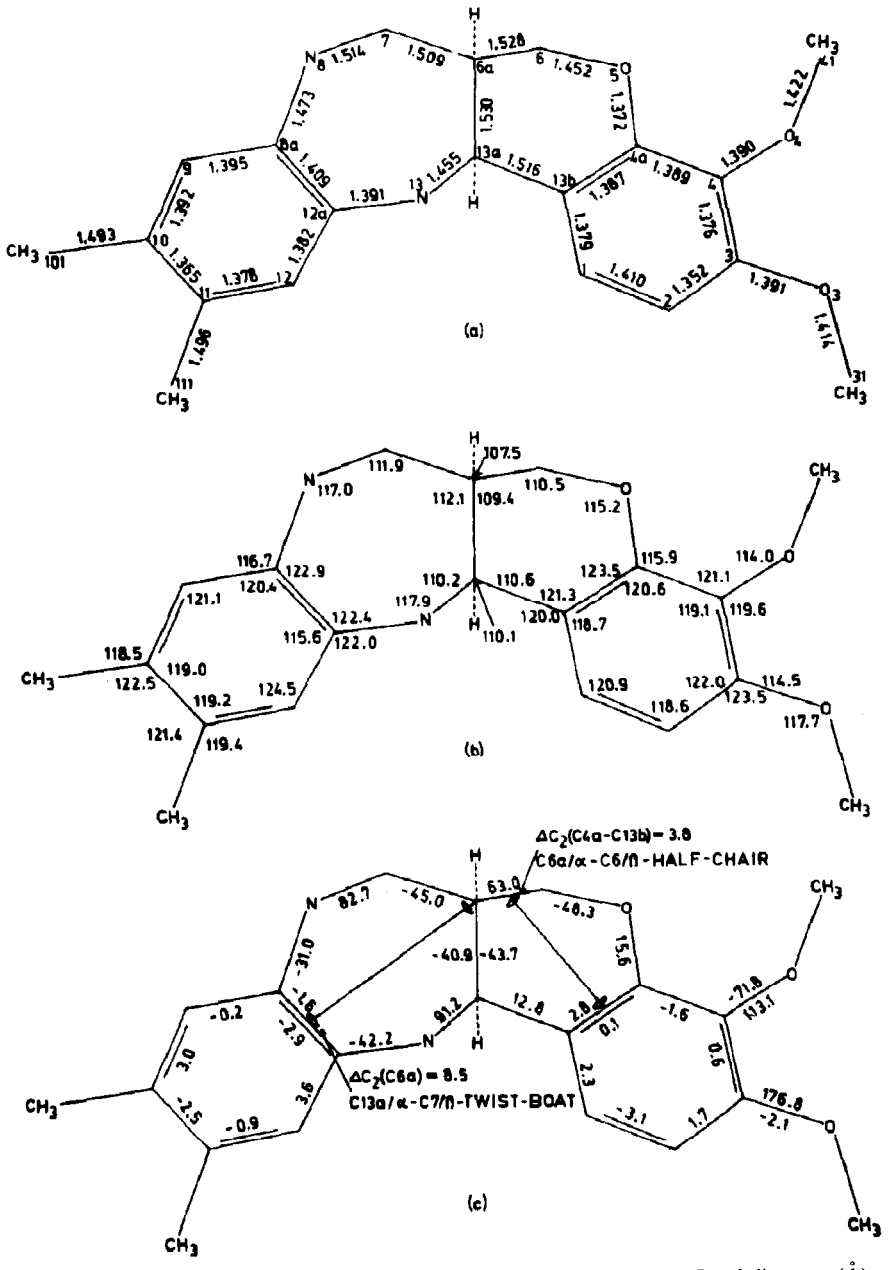

Fig. 3. Intramolecular dimensions of (6*aR*,13*aS*)3,4-dimethoxy-10,11-dimethyl-*cis*-HHCB. (a) Bond distances (Å); σ range = 0.007–0.012 Å. (b) Bond angles (°); σ range = 0.5–0.8°. (c) Endocyclic torsion angles (°); σ range = 0.8–1.2°.

romolecular systems can result in hypochromicity and/or bathochromicity being exhibited by absorption spectra, the spectroscopic behavior of ZIMET 54/79 and 55/79 was investigated in the absence and presence of liposomal model membranes. Between pH 6 and 8, both in phosphate-

Table 3

ZIMET substances derived from *trans*-HHCB (fig. 1, **3**) and *trans*-OHDCB (fig. 1, **4**) (substituents attached to the racemic images **rac-3** and **rac-4**, respectively) derivatives without antitumor activity

ZIMET no.	Substituents	Images
81/75	3-methoxy	**rac-3**
53/76	3,4-dimethoxy	**rac-3**
51/80	10,11-dimethyl	**rac-3**
72/78	3-methoxy-10,11-dimethyl	**rac-3**
19/78	3,4,10,11-tetramethoxy	**rac-3**
102/76	3,4-dimethoxy-10,11-dimethyl	**rac-3**
32/86	10,11-dimethyl	**rac-4**

buffered saline and when present in unbound form, both compounds exhibit absorption peaks with maxima at 210 and 303 nm. In the presence of EPC/Chol liposomes at a lipid/agent molar ratio of 7.7:1 (concentrations: ZIMET 54/79 and 55/79, 0.1 mM; EPC, 0.77 mM; Chol, 0.77 mM; in phosphate buffered saline), the long-wavelength absorption peaks of ZIMET 54/79 and 55/79 decreased by 9.1 and 5.5% at pH 7, respectively. Simultaneously, the long-wavelength maximum

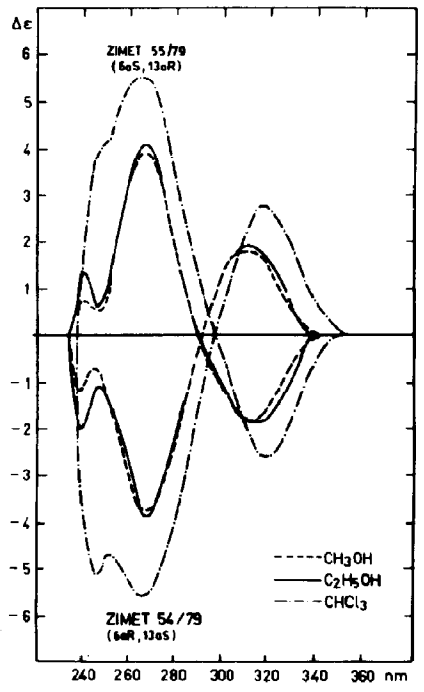

Fig. 4. CD curves of (6*aR*,13*aS*)-3,4-dimethyl-10,11-dimethyl-HHCB (ZIMET 54/79) and (6*aS*,13*aR*)-3,4-dimethyl-10,11-dimethyl-HHCB (ZIMET 55/79) in different solvents.

Table 4

Cotton effects and configurations of the enantiomeric couples ZIMET 54/79 and 55/79 (fig. 4), ZIMET 52/80 and 14/89, ZIMET 89/79 and 88/79, ZIMET 15/87, and 16/87 (fig. 5)

ZIMET no.	Formula (molecular weight)	Cotton effects (Ethanol)	(nm) Δε		Absolute configuration
54/79	$C_{20}H_{24}N_2O_3$ (340.4)	236 −1.2	266 −3.9	310 +1.8	(6*aR*,13*aS*)
55/79	$C_{20}H_{24}N_2O_3$ (340.4)	236 +0.8	266 +4.8	310 −1.8	(6*aS*,13*aR*)
52/80	$C_{18}H_{20}N_2O$ (280.4)	237 −1.0	274 −4.15	309 +1.7	(6*aR*,13*aS*)
14/89	$C_{18}H_{20}N_2O$ (280.4)	237 +0.7	274 +4.2	309 −1.8	(6*aS*,13*aR*)
89/79	$C_{18}H_{20}N_2O_3$ (312.4)	335 −1.5	265 −4.9	304 +2.25	(6*aR*,13*aS*)
88/79	$C_{18}H_{20}N_2O_3$ (312.4)	335 +1.25	265 +4.8	304 −2.2	(6*aS*,13*aR*)
15/87	$C_{20}H_{22}N_2O_3$ (338.4)		271 −28	306 +20.2	(6*aR*,13*aS*)
16/87	$C_{20}H_{22}N_2O_3$ (338.4)		271 +28	306 −20.8	(6*aS*,13*aR*)

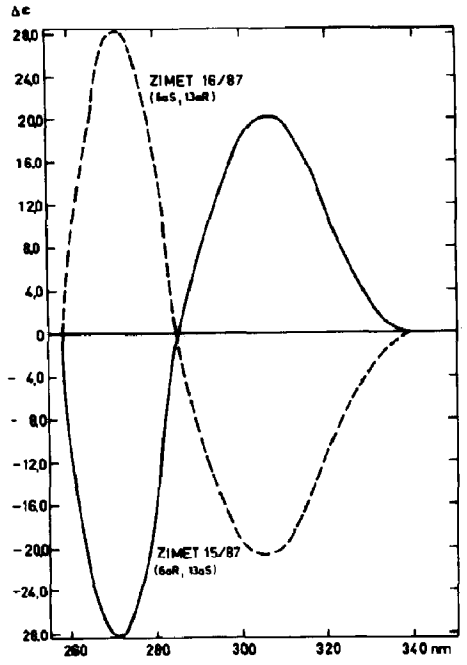

Fig. 5. CD curves of (6*aR*,13*aS*)-10,11-dimethyl-OHDCB (ZIMET 15/87) and (6*aS*,13*aR*)-10,11-dimethyl-OHDCB (ZIMET 16/87) in ethanol.

was shifted by about 3 nm from 303 to 306 nm. Such small hypochromic and bathochromic shifts may indicate that the interaction of these compounds with the phospholipid matrix of the liposomal model membranes is rather weak. In addition, significant differences were observed between the enantiomers ZIMET 54/79 and 55/79.

The agent-liposomal membrane model system lacks an intrinsic fluorophore. Hence, the environmentally sensitive fluorescent probe 1,8-ANS, capable of being inserted into the bilayer surface region [29], was used in the study of fluorescence. On insertion into multi-component lipid bilayer sites of low solvent accessibility, the quantum efficiency of the probe molecule for emission increases 30–40-fold compared to aqueous solution [30,31]. Hence, although the composition of this system was chosen such that the bilayer-embedded species constituted a minor proportion of the fluorophore concentration, the overall fluorescence emission arose predominantly from inserted probe molecules. The steady-state fluorescence data in table 5 demonstrate that the interaction with the agents exerts a considerable effect on the emission by membrane-bound 1,8-ANS. The relative decrease in intensity appears to be of the same order of magnitude on varying the composition of the system whilst maintaining the EPC/1,8-ANS (total concentration) ratio constant. In particular, no significant influence of the sign of the liposomal charge is evident whereas the extent to which the 1,8-ANS anion is incorporated responds in the expected manner [32]. No distinct differences in effect between the enantiomers were detected regarding interaction with the stereochemically unspecific model system. In order to elucidate the physical origin of the steady-state fluorescence effects, time-resolved studies were performed (data in table 6). By proper selection of the long wavelength emission range and using cholesterol-containing samples strongly limiting 1,8-ANS binding [30,32,33], we resolved two decay components which provide information on either probe species of interest. These are the moderately fluorescing bilayer-embedded species (determining γ_1 and τ_1) on the one hand and the very weakly fluorescent water-accessible species displaying a characteristic decay time of 0.2 ns [34] on the other (γ_2 and τ_2;

Table 5

Agent-induced relative decrease in fluorescence intensity of lipomally bound 1,8-ANS under various experimental conditions

Conditions: excitation wavelength, 370 nm; emission wavelength, above 520 nm; [EPC] and [Chol], 0.77 mM; [1,8-ANS], 0.02 mM; phosphate-buffered saline ([Na^+], 0.19 M; pH 7.2).

ZIMET no.	Liposome composition	Charge	[Benzodiazepine] (mM)	Relative decrease of fluorescence intensity (%)
54/79	EPC/Chol	0	0.04	7.5
55/79	EPC/Chol	0	0.04	11.0
54/79	EPC/Chol	0	0.058	9.1
55/79	EPC/Chol	0	0.058	5.5
54/79	EPC/Chol/DCP	−	0.04	9.3
55/79	EPC/Chol/DCP	−	0.04	8.3
54/79	EPC/Chol/SA	+	0.04	7.8

Table 6

Fluorescence decay data for 1,8-ANS in liposomal samples in the absence and presence of ZIMET 54/79

Conditions: excitation wavelength, 337 nm; emission wavelength, above 520 nm; [EPC] and [Chol], 0.77 nm; [1,8-ANS], 0.02 mM; [ZIMET 54/79], 0.04 mM; phosphate-buffered saline ([Na^+], 0.19 M; pH 7.2); T, 20.0 °C.

	ZIMET 54/79	
	Absent	Present
Decay time (ns)		
τ_1	6.10 (±0.05)	6.01 (±0.04)
τ_2	0.21 (±0.05)	0.19 (±0.02)
Pre-exponential factor		
γ_1	0.70	0.40
γ_2	0.30	0.60

table 6). In the presence of the agents, no significant change in τ_1 and τ_2 takes place, however, a strong shift in the ratio of the components in favour of the water-accessible species is observed. This is clearly indicative of the partial relocation of the probe from hydrophobic sites into a hydrophilic environment, as a consequence of the interaction of the agents with the liposomal membrane.

3.5. Activity of cis and trans diastereomers and cis enantiomers in the cyclic nucleotide system

Via in vitro experiments (table 7) it was found that micromolar levels of the *cis*-racemate ZIMET 101/76, *trans*-racemate 102/76 or of the *cis* enantiomers ZIMET 54/79 and 55/79 reduced the cAMP hydrolysing activity in fractions of L1210 cells. The inhibition of cAMP-PDE activity results in an increase in cAMP levels in leukemia L1210 cells (initial cAMP concentration, 2.1 μM). Quercetin and theophylline, both well known as cAMP-PDE inhibitors, when tested under identical experimental conditions, showed 2- and 8-fold higher I_{50} values, respectively, when compared with *cis*- and *trans*-HHCB derivatives.

On performing in vivo experiments (table 7), both the *cis*-racemate ZIMET 101/76 and the

Table 7

In vitro and in vivo effectiveness in the cyclic nucleotide system and decrease in L1210 cell number induced by two diastereomers (*cis*- and *trans*-racemates) and two *cis* enantiomers of selected chromeno[4,3-*b*][1,5]benzodiazepine derivatives

(In vitro) Inhibition of 'low-K_m' cAMP phosphodiesterase activity of L1210 soluble fractions from mice; I_{50}, concentration of inhibitor resulting in 50% inhibition of cAMP degradation on addition of the test compound and constant cAMP concentration. (In vivo) Increases in cAMP, cGMP, cAMP-PDE and cGMP-PDE activities, decrease in L1210 cell numbers/mouse. S, supernatant; P, precipitate; underlined numbers indicate significance.

ZIMET no./ respective standard compounds	Relative configuration	In vitro I_{50} (μM)	Dose (mg/kg)	cAMP (increase) (%)	cAMP-PDE activity (increase) (%)	Number of L1210 cells/mouse (decrease) (%)	cGMP (increase) (%)	cGMP-PDE activity (increase) (%)	
							S	S	P
Control		0	0	0	0	0	0	0	0
101/76	(±)*cis*	174.7	250	71.0	61.1	28.3			
			500	178.3	100.8	58.2	100	109	183
102/76	(±)*trans*	159.3	250	2.1	0	13.8			
			500	0	13.2	15.1	0	−17	55
54/79	(+)*cis*	185.0	125	38.0	79.3	48.8	−2.9	10.9	
			250	77.8	265.2	74.4	4.3	17.2	
			500	103.7	363.0	78.7	3.9	29.2	
55/79	(−)*cis*	178.0	125	8.7	13.4	17.5	1.4	−6.4	
			250	12.0	9.8	20.5	0	4.0	
			500	39.1	64.7	45.1	2.8	4.9	
Sarcolysin			0.3	73.5	140.9	59.4			
Quercetin		388.8							
Theophylline		1520.0							

(+)*cis* enantiomer ZIMET 54/79 were found to stimulate the activity of adenylate cyclase (not shown) as well as that of cAMP phosphodiesterase, with the overall increase in cAMP level of leukemia cells being considerable. In contrast, the *trans*-racemate ZIMET 102/76 displayed no effect at all, and the (−)*cis* enantiomer ZIMET 55/79 only a very slight influence in raising cAMP levels on administration at 500 mg/kg. The decrease in cell number for L1210 cells was significant in every case and was found to be greatest with ZIMET 101/76 and 54/79. Increases in both cGMP level and cGMP phosphodiesterase activity were unambiguously determined for ZIMET 101/76, however, the results for ZIMET 54/79 were inconclusive. The clinically used anticancer drug sarcolysin ((*R*,*S*)4-[bis(2-chloroethyl)amino]phenylalanine) at a comparatively tiny dose showed similar effects to those of ZIMET 101/76 and 54/79 in the cAMP system.

4. Discussion

The investigation of physico-chemical, biochemical and biological parameters of partially hydrogenated chromeno[4,3-*b*][1,5]benzodiazepine derivatives should help in the elucidation of the structural factors essential to the biological efficacy of this new class of antineoplastic agents. A thorough knowledge of structure-activity relationships and possible targets are two basic requirements in order to approach further developments in drug design. All data pertinent to achieving greater specificity of the agents are closely connected with the stereochemistry of chiral receptors or active sites in enzymes on the one hand, and chiral agents or drugs on the other. The conferring of specificity for a particular antigen to antibodies has thus far remained an unattainable objective of studies on drug-target interactions in the field of cancer chemotherapy. The two neighboring asymmetric carbon atoms in the heterocyclic ring systems described here offer the possibility of synthesizing two diastereoisomers with totally different molecular shapes which are readily distinguishable on NMR spectra as *cis* and *trans* configured HHCB (cf. fig. 1 and tables 1–3). The resolution of biologically active *cis* configured racemates into optically active enantiomers was an imperative requirement due to the expected differences in biological activities.

The determination of the absolute configurations of the enantiomers by X-ray diffraction and CD measurements allowed us to search more systematically for new active agents and to design new molecules based on a knowledge of the necessary substituents for hypothetically negative modeling of a receptor or active site in an enzyme.

The *cis* configuration initially established using NMR and the substitution on the heterocyclic ring system with methyl and methoxy groups have been confirmed via X-ray diffraction analysis. The conformation observed in crystals probably exists in biological systems as well. However, under the influence of stereochemically stable membrane constituents or active sites in enzymes, the conformation of the agents may be altered within certain limits.

Correlation of the absolute configuration (6*aR*,13*aS*) of ZIMET 54/79 with the Cotton effects in the CD spectrum allows us to compare this CD curve with those of analogous chromeno[4,3-*b*][1,5]benzodiazepine derivatives. However, there are examples in the literature [36] showing that similar, substituted tetrahydroisoquinolines with the same absolute configurations may give rise to opposite Cotton effects due to changes in conformation. The substituents on the compounds under discussion are located at remote, peripheral sites on the molecule, thereby exerting only a slight effect on the chiral center and conformational barriers. Nevertheless, the $\Delta\epsilon$ in CD curves of the dioxino-annellated compounds ZIMET 15/87 and 16/87 is 6–7-times greater (fig. 5) than those of *cis*-HCCB derivatives (fig. 4).

After elucidation of the physico-chemical properties and parameters of biologically active agents, their reactions with target cell membranes or receptors require to be established. Concerning tumor cell membranes, since we lack sufficient experience in the study and isolation of membrane compartments and receptor regions, our first approach was to investigate liposomal membrane

Table 8

Maximum increase in life span (ILS) of tumor-bearing mice and respective tumor weight inhibition (TWI) after treatment with antineoplastic chromeno[4,3-*b*][1,5]benzodiazepines

ZIMET no.	Dose (mg/kg)	Schedule [a]	Day	Tumor model [a,b]	Hybrids or strain of mice	Effect (%) [c]
101/78	500	9×i.p.	1–4 7–11	L1210 i.p.	$ABD2F_1$	107.3 ILS
	250	i.p.	1–4 7–11	P388 i.p.	$ABD2F_1$	67.2 ILS
	500	i.p.	1–4 7–11	LLC s.c.	$ABD2F_1$	69.5 TWI
54/79	250	4×i.p.	1–4	L1210 i.p.	$ABD2F_1$	124.3 ILS
	500	9×p.o.	1–4 7–11	L1210 i.p.	$ABD2F_1$	98.6 ILS
	250	4×i.p.	1–4	P388 i.p.	$ABD2F_1$	130.6 ILS
	500	9×i.p.	1–4 7–11	B16 i.p.	C57BL/6	108.1 ILS
	500	9×i.p.	1–4 7–11	$ABDt_2$ i.p.	$ABD2F_1$	97.0 ILS
	500	9×p.o.	1–4 7–11	$ABDt_2$ i.p.	$ABD2F_1$	6.0 ILS
	500	9×p.o.	1–4 7–11	LLC s.c.	$ABD2F_1$	69.4 TWI
31/86	500	9×i.p.	1–4 7–11	P388 i.p.	$B6D2F_1$	109.4 ILS
15/87	500	2×i.p.	1, 3	P388 i.p.	$B6D2F_1$	152.3 ILS
	250	2×p.o.	1, 3	P388 i.p.	$B6D2F_1$	90.6 ILS
	500	4×p.o.	1–4	LLC s.c.	$B6D2F_1$	94.8 TWI

[a] i.p., intraperitoneal; p.o., per os; s.c., subcutaneous.

[b] Inoculation of 5×10^6 (L1210) or 1×10^6 (P388) ascites cells, or 0.2 ml suspension of 10% B16 melanoma cells, or LLC in small pieces (≈ 3 mm diameter).

[c] All results are significant on the basis of confidence limits ($p = 5\%$).

interactions with biologically active and inactive agents.

The results of absorption and fluorescence studies show that the hydrophobic *cis*-HHCB derivatives have an affinity for liposomal membranes. Assertions concerning stereochemical aspects or mechanisms of action are not possible on the basis of these experiments as the liposomal constituents are achiral. On interaction with liposomal membranes, the agents appreciably perturb the ordered hydrophobic bilayer probe-binding site of 1,8-ANS. The small hypochromic and bathochromic shifts observed in absorption spectroscopy and the data on steady-state fluorescence (tables 5 and 6) are also interpreted along these lines. On the whole, our results provide evidence in support of the incorporation of agent into the membrane, probably via hydrophobic interaction, and indicate the possible involvement of membrane-directed processes in the cancerostatic action of ZIMET 54/79. Studies on drug-cell-membrane interactions were carried out in the very narrow context of evaluating the influence of antineoplastically active and inactive HHCB derivatives on the cyclic nucleotide system. The results on cAMP phosphodiesterase inhibition by a number of stereoisomers in vitro conflict with the findings for in vivo experiments which demonstrated activation of the entire adenylate cyclase system. In vitro as well as in vivo, enhancement of cAMP levels was observed, albeit via different mechanisms. The diastereoisomeric and enanti-

omeric configurations of the compounds were not distinguishable in the in vitro experiments. The findings in vivo show that the activity in the cAMP system is correlated with the (+)*cis* configuration (6*aR*,13*aS*) of the heterocyclic ring system. The decrease in cell number for mouse L1210 cells, which was significant for all configurations, was distinctly larger with (+)*cis* configured compounds.

Although quercetin and theophylline do not exhibit antineoplastic activity like sarcolysin, they do inhibit the degradation of cAMP. It is unclear whether the enhancement in cAMP levels of L1210 cells from mice (table 7) is the cause or merely a result of the inhibition of malignant cell growth. Neither *cis* nor *trans* configuration agents showed antimicrobial activity against Gram-positive or Gram-negative bacteria, yeasts, fungi, and mycobacteria. Furthermore, neither structure was able to induce λ-prophages in lysogenic cells of *Escherichia coli* K12 (λ-28) or to inhibit the multiplication of λ-phages in *E. coli* C600 (BIP test). In conclusion, no growth inhibitory effects were observed for any *cis* or *trans* stereoisomers when tested against a wide spectrum comprising 19 microorganisms and in two special test models. We therefore suggest that direct interaction of the compounds with DNA/RNA metabolism and/or its regulation, as has been shown for well-known alkylating agents, does not take place.

Of the agents that were tested with respect to L1210 or P388 leukemia (tables 1–3), only (+)*cis* configured structures with 10,11-dimethyl substituents and oxygen at positions 3,4 (table 1) and 1,4 (table 2), respectively (ZIMET 101/76, 54/79, 31/86, and 15/87), were found to be active against experimental tumors. The in vitro effectiveness of ZIMET 20/78 ((±)*cis*-3,4,10,11-tetramethoxy derivative, table 1) could not be confirmed for the in vivo situation. (−)*cis* and (±)*trans* configured molecules as well as heterocycles lacking substituents at positions 3, 4, 10 and 11 proved to be inactive (tables 1–3). Table 8 lists data on the maximum increase in life span of tumor-bearing mice and tumor weight inhibition, respectively, determined with ZIMET 101/76, 54/79, 31/86 and 15/87; for example, 107.9% ILS denotes the absolute value in comparison with 0% therapeutic

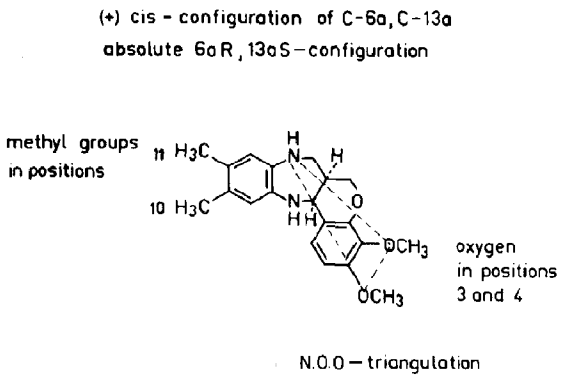

Fig. 6. Structural requirements for antitumor activity.

effect for controls. The effective doses (mg/kg) are relatively high, but were tolerated well.

Fig. 6 illustrates the structural requirements for *cis*-HHCB and *cis*-OHDCB derivatives to be active upon antitumor models and the cyclic nucleotide system. The reason for the importance of the hydrophobic methyl groups at positions 10 and 11 is unclear. The requirement of two oxygen atoms at positions 3 and 4 is in accordance with hypothetical N · O · O triangulation (fig. 6) postulated initially by Zee-Cheng and Cheng [37,38] as a molecular pattern for antileukemic drugs. The absolute configuration (6*aR*,13*aS*) of the asymmetric carbon atoms is an unequivocal requirement for interaction with chiral active sites in enzymes, unknown receptors at the cell membrane, or other cell constituents.

Fig. 7 represents a projection of the molecule, showing its shape with the conformation in a crystal as analyzed by X-ray diffraction, for the case of a hypothetical pocket in an enzyme.

Continued improvements in the development of structure-activity characteristics are aimed at the creation of a negative model for a conceivable agent-receptor interaction site. The (−)*cis* and (±)*trans* configured ring systems obviously do not fit well at the active sites in enzymes. The absence of substituents in positions 10 and 11 or the loss of methoxy or 3,4-ethylenedioxy groups resulted in the activity of the agent vanishing in our antitumor test systems. In terms of the evaluation of this new class of heterocyclic antitumor

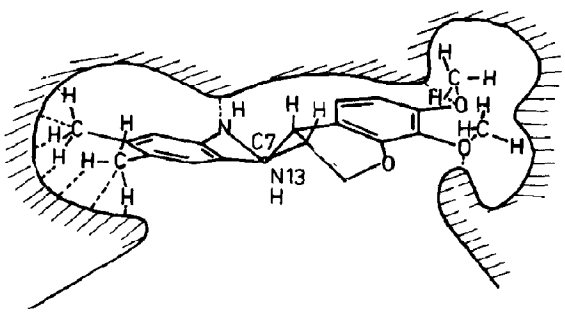

Fig. 7. Hypothetical interaction between (6*aR*,13*aS*)3,4-dimethoxy-10,11-dimethyl-HHCB (ZIMET 54/79) and the active center of an enzyme or with a receptor.

agents, it is of interest that the biologically active ZIMET 54/79 did not show any significant psychotropic (E. Rostock, personal communication) or immunosuppressive (R. Grupe, personal communication) activity. Furthermore, acute toxicity has been determined in mice by intraperitoneal and oral administration routes. The LD_{50} value was reported to be 2.5 g/kg body weight intraperitoneally. Per os the mice tolerated 5 g/kg (H. Hoffmann, personal communication). These results in the context of the administered doses (table 8) suggest that the agents are less toxic than most antitumor drugs currently in clinical use. The necessity for administration of high doses demands the designing of agents with greater bioavailability, and/or biological activity at lower dose levels. An increase in hydrophilicity of the agents via incorporation of hydrophilic substituents should lead to a better balancing of the pronounced hydrophobicity and promote bioavailability. Elucidation of the pertinent target in tumor cell membranes or cell organelles should help in contributing to greater understanding of the mode of action.

Acknowledgements

We wish to thank Mrs. Helgardt Gemeinhardt, Ulrike Gröbner, Kristine Müller and Ursula Zscherpe for experimental assistance and Dr. Günter Reck, Berlin, for performing X-ray diffraction analysis.

References

1 W. Losert, Pharmazie 28 (1973) 351.
2 R. Schauer, Angew. Chem. 84 (1972) 41.
3 M.S. Amer and W.E. Kreighbaum, J. Pharm. Sci. 64 (1975) 1.
4 J.A. Nathanson and J.W. Kebabian, Cyclic nucleotides I and II (Springer, Berlin, 1982).
5 J. Otten, J. Bader, G.S. Johnson and Ira Pastan, J. Biol. Chem. 247 (1972) 1632.
6 J. Otten, G.S. Johnson and I. Pastan, Biochem. Biophys. Res. Commun. 44 (1971) 1192.
7 Z.P. Horowitz, B. Beer, D.E. Clody, J.R. Vogel and M. Chasin, Psychosomatics 13 (1972) 85.
8 J.S. Driscoll, N.M. Melnick, F.R. Quinn, N. Lomax, J.P. Davignon, R. Ing, B.J. Abott, G. Congleton and L. Dudeck, Cancer Treat. Rep. 62 (1978) 45.
9 W.A. Remers, Antineoplastic agents (Wiley, New York, 1984).
10 W. Werner, W. Jungstand, W. Gutsche, K. Wohlrabe, W. Römer and D. Tresselt, Pharmazie 34 (1979) 394.
11 W. Werner, K. Wohlrabe, W. Gutsche, W. Jungstand and W. Römer, Fol. Haematol. 108 (1987) 637.
12 W. Werner and G. Burckhardt, J. Prakt. Chem. 328 (1986) 713.
13 W. Werner, K. Wohlrabe, Iduna Fichtner and W. Wohlrab, Arch. Geschwulstforsch. 57 (1987) 17.
14 W. Werner, W. Gutsche and J. Baumgart, Akademie der Wissenschaften der DDR, DD Pat. 266356 A1 (25.11.1987).
15 A. Messerschmidt and W. Werner, Crystallogr. Struct. Commun. 10 (1981) 1053.
16 W.S. Singleton, M.S. Gray, M.L. Brown and J.L. White, J. Am. Oil Chem. Soc. 42 (1965) 53.
17 H. Hanschmann and G. Löber, Stud. Biophys. 117 (1987) 61.
18 E. Stutter and K. Geller, in: Texte zur Physik, eds. E. Klose and B. Wilhelmi (Teubner, Leipzig, 1986) vol. 10, p. 81.
19 H. Schütz, E. Stutter, K. Weller and I. Petri, Stud. Biophys. 104 (1984) 23.
20 W.J. Thompson and M.M. Appleman, Biochemistry 10 (1971) 311.
21 A.G. Gilman, Proc. Natl. Acad. Sci. U.S.A. 67 (1970) 305.
22 W.F. Fleck, Post. Hig. Med. Doswiadeczalnej 28 (1974) 479.
23 W. Gutsche, W. Schulze, W. Jungstand and K. Wohlrabe, Pharmazie 38 (1983) 105.
24 W. Schulze, W. Jungstand, W. Gutsche, K. Wohlrabe and G. Horn, Pharmazie 33 (1978) 111.
25 J. Baumgart, J. Güttner, E. Zborowska and A. Czarnomska, Arch. Geschwulstforsch. 58 (1988) 223.
26 W. Gutsche and W. Wohlrab, Dermatol. Monatsschr. 169 (1983) 509.
27 W. Jungstand, Fol. Haematol. 108 (1981) 644.
28 W.L. Duax, C.M. Weeks and D.C. Rohrer, in: Topics in stereochemistry, eds. E.L. Eliel and N. Allinger (Wiley, New York, 1976) vol. 9, p. 271.
29 W. Lesslauer, J. Cain and J.K. Blasie, Biochim. Biophys. Acta 231 (1971) 547.

30 D.H. Haynes and H. Staerk, J. Membrane Biol. 17 (1974) 313.
31 J. Slavik, Biochim. Biophys. Acta 694 (1982) 1.
32 H. Hanschmann, K. Geller, E. Stutter and G. Löber, Stud. Biophys. 128 (1988) 51.
33 K. Geller, E. Stutter, H. Hanschmann, G. Löber, H. Schütz and E. Birckner, Stud. Biophys. 117 (1987) 67.
34 G.W. Robinson, R.J. Robbins, G.R. Fleming, J.M. Morris, A.E.W. Knight and R.J.S. Morrison, J. Am. Chem. Soc. 100 (1978) 7145.
35 W. Römer and W. Werner, Pharmazie 37 (1982) 382.
36 G. Snatzke, Angew. Chem. 91 (1979) 392.
37 K.Y. Zee-Cheng and C.C. Cheng, J. Pharm. Sci. 59 (1970) 1630.
38 C.C. Cheng and R.K.Y. Zee-Cheng, Heterocycles 15 (1981) 1275.
39 C.K. Johnson, ORTEP Report ORNL-3794 (Oak Ridge Natl. Lab., TN, 1965).